24th IMEKO TC4 International Symposium
22nd International Workshop on ADC and DAC Modelling and Testing
IMEKO TC-4 2020
Palermo, Italy, September 14-16, 2020

# High sensitivity Nitrogen-Vacancy-assisted magnetic/electric field sensing at INRIM

E. Moreva[1], E. Bernardi[1], V. Pugliese[2], P. Traina[1], A. Sosso[1], S. Ditalia Tchernij[2,3], J. Forneris[2,3], F. Picollo[2,3], G. Petrini[2,1], Z. Pastuovic[4], I. P. Degiovanni[1], P. Olivero[2,5,3,1], M. Genovese[1,3]

[1]*Istituto Nazionale di Ricerca Metrologica, Strada delle cacce 91, Torino, Italy, m.genovese@inrim.it*
[2]*Physics Department - University of Torino, Torino, Italy*
[3]*Istituto Nazionale di Fisica Nucleare (INFN) Sez. Torino, Torino, Italy*
[4]*Centre for Accelerator Science, Australian Nuclear Science and Technology Organisation,New Illawarra rd., Lucas Heights, NSW 2234, Australia*
[5]*NIS inter-departmental centre - University of Torino, Torino, Italy*

***Abstract* – Nitrogen-vacancy centers in diamond allow measurement of enviromental properties such as magnetic and electric fields at nanoscale. The working principle is based on the measurement of the resonance frequency shift of Nitrogen-vacancy centers, detected by monitoring the photoluminescence of one single center or an ensemble of them. Here we present a high sensitivity magnetometry technique, based on lock-in detection, with particular features required for biological applications.**

## I. INTRODUCTION

High sensitivity magnetometry is of great importance for several research fields, for instance, biological science and medicine. Magnetic sensing techniques are employed to map brain activity[25, 2, 3, 4] or measure the magnetic field produced by electrical currents in the heart[5]. Magnetometers based on NV centers in diamond represent a valid alternative to existing devices, and they can lead to a new generation of non-invasive detection methods. Indeed, their biocompatibility [6, 26, 8, 9, 10, 11] and efficiency at room temperature are important advantages for this kind of applications. Also, a low optical power and a small sensing volume are necessary to extend NV-magnetometry to single living cells.

The presented work is characterized by a sensing volume of 1 $\mu$m$^3$, that will allows intercellular resolution. An optical power of 80 mW is applied for $\tau_{means} = 10$ ms. A cell can probably not sustain this value of optical irradiance, but using this power is possible to define a lower bound to biocompatible sensitivity.

In the NV centers electronic ground state, the application of a magnetic field removes the degeneration between $m_s = \pm 1$ spin states. Their separation in frequency is proportional to the component $B_{NV}$ of the field along the NV-axis:

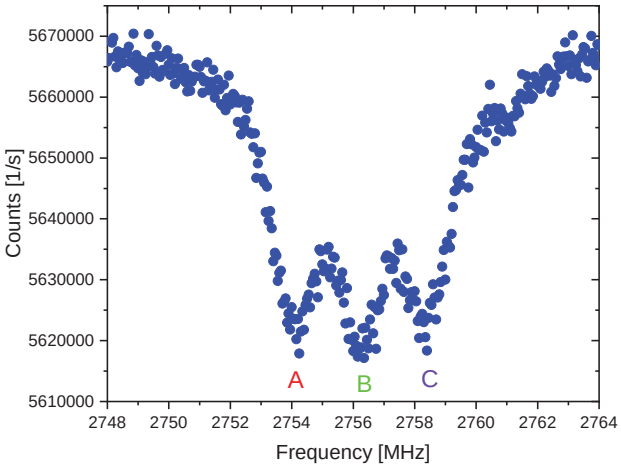


*Fig. 1. ODMR spectrum of an ensemble of NV centers. The three dips due to the Hyperfine Coupling with $^{14}N$ nucleus are labelled with the letters A,B,C*

$$h\Delta\nu = 2g\mu_B B_{NV} \tag{1}$$

where $g$ is the g-factor and $\mu_B$ the Bohr magneton. This two states present a decrease in the photoluminescence with respect to $m_s = 0$ state. To detect this phenomenon, NV centers have to be driven by microwave of a particular frequency of 2.87 GHz: this technique takes the name of Optically Detected Magnetic Resonance (ODMR)[12, 13, 14, 15]. An example of ODMR spectrum is presented in Fig. 1, where it is possible to note the three dips structure due to the hyperfine coupling with the $^{14}$N nucleus. The application of a magnetic field will shift the ODMR spectrum, and so the applied magnetic field can be measured detecting the shift in the ODMR spectrum[16, 17, 18, 19].

## II. EXPERIMENTAL

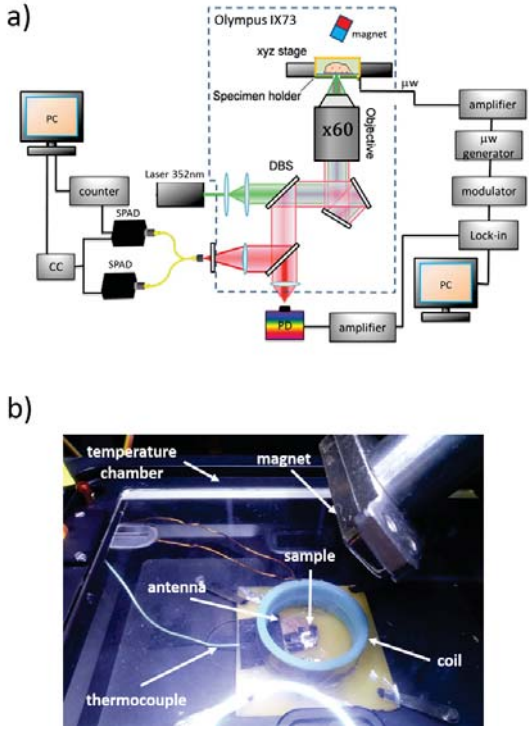


*Fig. 2. (a) Schematic representation of the implemented setup. The optical excitation using a green laser, the microwave($\mu w$) control, the collection of the red photoluminescence and the lock-in detection are depicted. (b) Image of the diamond sample and of controlled temperature chamber. The permanent magnet and the coil for the magnetic control are also shown.*

Our setup consists of an inverted microscope, adapted to confocal measurements with single-photon sensitivity, see Fig. 2 The sensor consists of a CVD diamond sample by Element Six of dimension $3 \times 3 \times 0.3$ mm$^3$. The sensing volume is 10 nm thick layer of NV centers at a depht of 15 nm with a concentration of $n_{[NV]} = 3 \times 10^{19} cm^{-3}$.

The diamond sample was mounted on a microwave planar ring antenna. The microwave control was obtained by a commercial microwave(MW) generator, whose central frequency was internally modulated a frequency $f_{mod}$. The output MW signal was amplified and then sent to the microwave antenna. Excitation light at 532 nm was focused on the bottom side of the diamond sample through an air objective. The emitted photoluminescence (PL), spectrally filtered with notch and long-pass filter at 650 nm, was collected and detected with two different acquisition systems. The 4% of the total PL was sent on a single photon detector (SPD). The signal from the SPD was used for the ODMR spectrum acquisition. The remaining 96% of the emitted PL was collected by NA=0.25 objective (Olympus 10×) and imaged onto a bias photodetector. The signal from the photodiode was sent to the input channel of a lock-in amplifier (LIA). A signal generator gives the reference signal for the lock-in amplifier and for the frequency modulation of MW. An external magnetic field was applied to the diamond sample using a permanent magnet fixed on a translation stage, allowing micrometric movement along the three spatial axes. The sample is located in a temperature controlled chamber.

The modulating signal is centered at the resonance dip and has an amplitude equal to the full- width half maximum of the resonance, see Fig. 3 (a). This implies that the resulting photoluminescence signal read by the LIA is also modulated at the same frequency. As depicted in Fig. 3 (b), the demodulated LIA signal present a linear zone centered around the dip of the original ODMR spectrum. In this region, a shift in the ODMR spectrum results in a linear change of the LIA signal. This implies that a change in the applied magnetic field, causing a linear shift in the ODMR spectrum, results in a linear change in the LIA signal[20, 21, 22].

## III. RESULTS

In Fig. 4 (a) is plotted the LIA signal in function of the MW frequency, for the same resonances considered in Fig. 1. There are three zones where the LIA signal is directly proportional to the resonance shift and hence to the applied field. The figure of merit of the LIA detection method is the slope of the curve in the linear zone.

Addressing all the three resonances simultaneously is possible to increase the slope of the curve of a factor 2[27]. For simultaneous hyperfine driving, the MW was mixed via a double-balanced mixer with a 2.16 MHz sinewave to create three simultaneous driving modulated frequencies near the central frequency. In this way, three frequency modulated MW tones separated by the hyperfine splitting $A_\perp = 2.16$ MHz are sent to the sample. When the center tone is at the frequency of the center resonances, all three resonance are excited and the slope of the curve is enhanced. An example of LIA spectrum for multiple frequency excitation is presented in 4 (b). With this method a magnetic sensitivity of $42.9 \pm 1.9$ nT/Hz$^{1/2}$ was obtained.

Furthermore, NV defects can be used like temperature sensors. A change of temperature causes a shift in the ODMR spectrum, but in this case the two dips, corresponding to $m_s = \pm 1$ spin states, shift in the same direction. The effect of temperature and magnetic field can be decoupled addressing both dips simultaneously but with the oppurtune phase differences wojciechowski2018precision. In alternative, by adopting a simple continuous-wave lock-in based technique and a field aligned orthogonal to NV axis [24], it is possible to reach an unprecedented temperature sensitivity value of $4.8$mK/Hz$^{1/2}$ in $\mu$m$^3$, in an appropriate no magnetic sensitive regime. It has to be underlined that, in order to do temperature measurement with micrometric

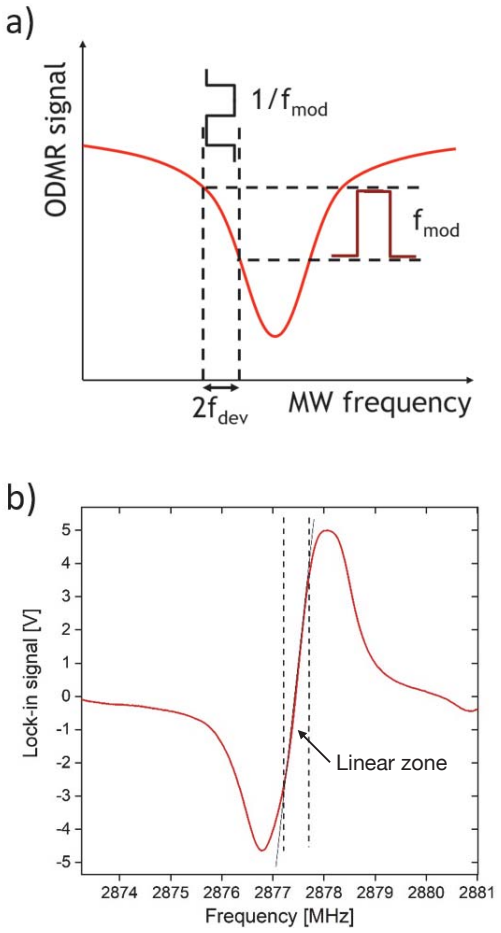


*Fig. 3. (a) Schematics of the lock-in detection technique. The microwave signal is frequency modulated with an ampltude $f_{dev}$ at a frequency $f_{mod}$. $f_{dev}$ is equal to the full-width half maximum of the orignal ODMR signal. The resulting photoluminescence signal will be also modulated at frequency $f_{mod}$. (b)Schematics of the lock-in amplifier (LIA) signal coming from the demodulation of the photoluminescence signal. The LIA signal present a minimum and a maximum corresponding to the microwave frequencies of maximum slope in the original ODMR signal, and a linear zone between these two points.*

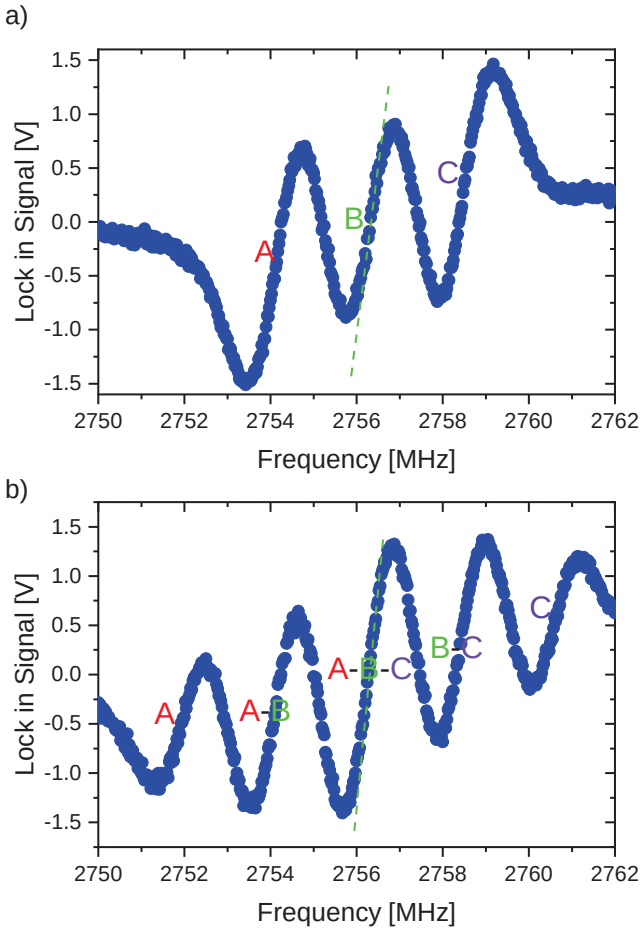


*Fig. 4. Lock-in spectrum of an ensemble of NV centers. (a) Single frequency excitation, the linear regions labelled with letters A,B,C corresponds to the dips in Fig. 1(b) Simultaneous Hyperfine driving, exciting simultaneously with three frequencies, all the three dips are excited when the center frequency corresponds to the central dips, and hence the slope of the curve is enhanced*

resolution, the bulk diamond has probably to be replaced by nanodiamonds. Due to the high thermal conductivity of diamond, the temperature measured by the sensor relaxes very fast to the temperature of the entire diamond substrate.

## IV. CONCLUSIONS

We presented an experimental set-up for the measurement of magnetic fields and temperature. The technique presented is based on the physical properties of the NV center and use lock-in detection in order to improve the sensitivity. This technique can be further improved, achieving even lower values of sensitivity, leading to measurement of magnetic field in biological systems at an intercellular scale.


## ACKNOWLEDGEMENTS

This work has received funding from the European Union's PATHOS EU H2020 FET-OPEN grant no. 828946 and Horizon 2020 and the EMPIR Participating States in the context of the projects EMPIR-17FUN06 "SIQUST" and 17FUN01 BeCOMe, from the project Piemonte Quantum Enabling Technologies (PiQuET), funded by the Piemonte Region within the Infra-P scheme (POR FESR 2014-2020 program of the European Union), from Departments of Excellence Project (L. 232/2016), funded by MIUR, from Coordinated Research Project F11020 of the

International Atomic Energy Agency (IAEA). The authors wish to thank Elio Bertacco and Giulia Tomagra.

REFERENCES

[1] J. Xiong, P. T. Fox, and J.-H. Gao, “Directly mapping magnetic field effects of neuronal activity by magnetic resonance imaging”, Human brain mapping, vol.20, No.1 pp.41-49, 2003.

[2] B. Li, J. P. Virtanen, A. Oeltermann, C. Schwarz, M.A. Giese, U. Ziemann, and A. Benali, “Lifting the veil on the dynamics of neuronal activities evoked by transcranial magnetic stimulation”, Elife, vol.6, pp.e30552, 2017.

[3] D.M. Kullmann, "Neurological channelopathies", Annual review of neuroscience, vol.33, pp.151-172, 2010.

[4] S.G. Waxman, "Axonal conduction and injury in multiple sclerosis: the role of sodium channels", Nature Reviews Neuroscience vol. 7, No 12, pp. 932?941, 2006.

[5] D. Cohen, “Magnetic fields around the torso: production by electrical activity of the human heart”, Science, vol.156, No.3775, pp.652-654, 1967.

[6] G. Tomagra, et al, “Quantal release of dopamine and action potential firing detected in midbrain neurons by multifunctional diamond-based microarrays”, Frontiers in neuroscience, vol.13, pp. 288, 2019.

[7] S.-J. Yu, M.-W. Kang, H.-C. Chang, K.-M. Chen, and Y.-C.Yu, "Bright fluorescent nanodiamonds: no photobleaching and low cytotoxicity”, Journal of the American Chemical Society, vol.127, No.50, pp.17604-17605, 2005.

[8] Y. Zhu, J. Li, W., Y. Zhang, X. Yang, N. Chen, Y. Sun, Y. Zhao, C. Fan, Q. Huang, "The biocompatibility of nanodiamonds and their application in drug delivery systems", Theranostics, vol. 2, No. 3, pp. 302, 2012.

[9] L. Guarina et al., "Nanodiamonds-induced effects on neuronal firing of mouse hippocampal microcircuits", Scientific Reports vol. 8, No. 1, pp. 1-14, 2018.

[10] A.M. Schrand, H. Huang, C. Carlson, J.J. Schlager, E. O?sawa, S.M. Hussain, L. Dai, "Are diamond nanoparticles cytotoxic" The journal of physical chemistry B, vol. 111, No. 1, pp. 2-7, 2007.

[11] K.-K., Cheng, C.-L. Liu, C.-C. Chang, J.-I Chao, "Biocompatible and detectable carboxylated nanodiamond on human cell", Nanotechnology, vol. 18, No 32, pp. 325102, 2007.

[12] A. Gruber, A. Drabenstedt, C. Tietz, L. Fleury, J. Wrachtrup, C. Von Borczyskowski, "Scanning confocal optical microscopy and magnetic resonance on single defect centers", Science, vol. 276, No 5321, pp. 2012-2014, 1997.

[13] P. Neumann, J. Beck, M. Steiner, F. Rempp, H. Fedder, P.R. Hemmer, J. Wrachtrup, F. Jelezko, "Single-shot readout of a single nuclear spin", Science, vol. 329, No 5991, pp. 542-544, 2010.

[14] L. Robledo, L. Childress, H. Bernien, B. Hensen, P.F. Alkemade, R. Hanson, "High-fidelity projective readout of a solid-state spin quantum register", Nature, vol. 477, No. 7366, pp. 574-578, 2011.

[15] L. Childress, M.G. Dutt, J. Taylor, A. Zibrov, F. Jelezko, J. Wrachtrup, P. Hemmer, M. Lukin, "Coherent dynamics of coupled electron and nuclear spin qubits in diamond", Science, vol. 314, No 5797, pp. 281-285, 2006.

[16] L.Rondin, J.-P. Tetienne, T. Hingant, J.-F. Roch, P. Maletinsky, V. Jacques, "Magnetometry with nitrogen-vacancy defects in diamond", Reports on progress in physics, vol. 77, No. 5, pp. 056503, 2014.

[17] J. Taylor, P. Cappellaro, L. Childress, L. Jiang, D. Budker, P. Hemmer, A. Yacoby, R. Walsworth, M. Lukin, "High-sensitivity diamond magnetometer with nanoscale resolution", Nature Physics, vol. 4, No. 10, pp. 810-816, 2008.

[18] J.R. Maze et al., "Nanoscale magnetic sensing with an individual electronic spin in diamond", Nature, vol. 455, No. 7213, pp. 644-647, 2008.

[19] K.Fang, V.M. Acosta, C. Santori, Z. Huang, K.M. Itoh, H. Watanabe, S. Shikata, R.G. Beausoleil, "High-sensitivity magnetometry based on quantum beats in diamond nitrogen-vacancy centers" , Physical review letters vol. 110, No 13, pp. 130802, 2013.

[20] R.S. Schoenfeld, W. Harneit, "Real time magnetic field sensing and imaging using a single spin in diamond" Physical review letters, vol. 106, No 3, pp. 030802, 2011.

[21] H.A. El-Ella, S. Ahmadi, A.M. Wojciechowski, A. Huck, U.L. Andersen, "Optimised frequency modulation for continuous-wave optical magnetic resonance sensing using nitrogen-vacancy ensembles" Optics express, vol. 25, No. 13, pp. 14809-14821, 2017.

[22] A.M. Wojciechowski, M. Karadas, C. Osterkamp, S. Jankuhn, J. Meijer, F. Jelezko, A. Huck, U.L. Andersen, "Precision temperature sensing in the presence of magnetic field noise and vice-versa using nitrogen-vacancy centers in diamond" Applied Physics Letters, vol. 113, No. 1, pp. 013502, 2018.

[23] J. F. Barry, M. J. Turner, J. M. Schloss, D. R. Glenn, Y. Song, M. D. Lukin, H. Park, and R. L. Walsworth, “Optical magnetic detection of single-neuron action potentials using quantum defects in diamond”, Proceedings of the National Academy of Sciences, vol.113, No.49, pp.14133-14138, 2016.

[24] Moreva et al., “Practical applications of quantum sensing: a simple method to enhance sensitivity of nitrogen-vacancy-based temperature sensors”, Physical Review Applied, vol. 13, No. 5, pp. 054057, 2020.

[25] J. Xiong, P.T. Fox, and J.-H. Gao, “Directly mapping magnetic field effects of neuronal activity by magnetic

resonance imaging", Human brain mapping, vol.20, No.1 pp.41-49, 2003.

[26] S.-J. Yu, M.-W. Kang, H.-C. Chang, K.-M. Chen, and Y.-C. Yu, "Bright fluorescent nanodiamonds: no photobleaching and low cytotoxicity", Journal of the American Chemical Society, vol.127, No.50, pp.17604-17605, 2005.

[27] J. F. Barry, M. J. Turner, J. M. Schloss, D. R. Glenn, Y. Song, M. D. Lukin, H. Park, and R. L. Walsworth, "Optical magnetic detection of single-neuron action potentials using quantum defects in diamond", Proceedings of the National Academy of Sciences, vol.113, No.49, pp.14133-14138, 2016.